

# Spatial Correlation of Spherical Polyelectrolyte Brushes in Salt-Free Solution As Observed by Small-Angle X-ray Scattering

Q. de Robillard, X. Guo, and M. Ballauff\*

*Polymer-Institut, Universität Karlsruhe, Kaiserstrasse 12, 76128 Karlsruhe, Germany*

T. Narayanan

*ESRF, BP 220, F-38043 Grenoble Cedex, France*

*Received August 4, 2000; Revised Manuscript Received September 12, 2000*

**ABSTRACT:** We report on the observation of spatial correlation of linear polyelectrolyte chains attached to latex particles. The particles are dispersed in water and consist of a solid poly(styrene) core and a shell of poly(acrylic acid) (PAA). At low pH the PAA chains are virtually uncharged, but full ionization can be reached for  $\text{pH} > 10$ . Small-angle X-ray scattering (SAXS) reveals an additional peak in the region of intermediate scattering angles when the chains are fully charged whereas no signal is seen in the uncharged state (low pH). Also, the peak is only seen if the polyelectrolyte chains attached to different particles overlap sufficiently. The position of the maximum scales with the square root of the particle concentration. The peak vanished when the ionic strength is raised by adding salt to the suspension. We assigned this signal to the weak maximum of the scattering intensity seen by small-angle scattering experiments in solutions of free linear polyelectrolytes ("polyelectrolyte peak"). The present investigation demonstrates that the same spatial correlation may occur when the polyelectrolyte chains are attached to the surface of colloidal particles.

## Introduction

The solution properties of polyelectrolyte differ markedly from those of uncharged macromolecular systems. This is due to the presence of charges along the chain which leads to long-range Coulombic interactions between the polymer segments.<sup>1–5</sup> If an excess of low-molecular-weight salt is added to solutions, the Coulombic forces are strongly screened. In this case the solution behavior of these systems can be compared to results obtained from uncharged macromolecules.<sup>1–3</sup> Dilute polyelectrolyte solutions without added salt, however, exhibit a totally different behavior. Static scattering experiment have revealed a maximum of the scattering intensity  $I(q)$  ( $q = (4\pi/\lambda) \sin(\theta/2)$ ;  $\lambda$  = wavelength of the used radiation and  $\theta$  = scattering angle) at a certain  $q^*$ . This "polyelectrolyte peak" has been the subject of numerous theoretical<sup>4–9</sup> and experimental<sup>4,5,10–15</sup> studies. A survey of experimental data shows that  $q^*$  scales with the polyelectrolyte concentration  $c_p$  as  $c_p^{1/2}$  in the semidilute regime and with  $c_p^{1/3}$  in the dilute regime (see for example the discussion of this point by Borsali et al.).<sup>14</sup> Moreover, the scattering intensity  $I(q^*)$  at the maximum decreases with increasing concentration of added salt.<sup>4,5</sup> This phenomenon has hence been attributed to the presence of long-range electrostatic interactions which impose a local order onto the polyelectrolyte solution.

There is no generally accepted model that satisfactorily explains all the features of salt-free polyelectrolyte solutions so far. An overwhelming number of recent experimental studies demonstrate, however, that the "polyelectrolyte peak" is a genuine feature of salt-free polyelectrolyte solution (see the discussions in refs 4, 5, and 13–15).

If linear polyelectrolyte chains can build up spatial structures in salt-free solutions which lead to a maximum of  $I(q)$ , the same phenomenon should in principle occur in systems in which the polyelectrolyte chains are

bound to solid surfaces. Such polyelectrolyte brushes consisting chains grafted densely to planar or curved surfaces have attracted much attention recently.<sup>16–28</sup> Interactions between polyelectrolyte chains should become observable when attaching such macromolecules to the surface of well-defined colloidal particles. Hence, scattering experiments on suitable spherical brushes of colloidal dimensions should reveal whether chains attached to surfaces lead to a similar ordering as observed in salt-free solutions of free polyelectrolyte chains.

Colloidal particles with attached polyelectrolyte chains can be achieved through adsorption of block copolymers on latex particles (see e.g. refs 24 and 25). Micellization of suitable block copolymers may lead to spherical micelles with a hydrophobic core and a corona consisting of polyelectrolyte chains.<sup>29–34</sup> These systems could be compared to star-branched polyelectrolytes in which polyelectrolyte chains emanate from a well-defined core.<sup>35,36</sup>

We have developed a method whereby linear polyelectrolyte chains can be grafted to the surface of well-defined core latex particles.<sup>37,38</sup> The synthesis proceeds through photoemulsion polymerization in which radicals are generated on the surface of monodisperse latex particles of radius  $R$  by photoinitiation.<sup>37</sup> These radicals start the polymerization of water-soluble monomers as for example acrylic acid (AA) directly on the surface, and the contour length  $L_c$  of the resulting poly(acrylic acid) (PAA) and their grafting density  $\sigma$  can be varied within wide limits.<sup>38</sup> Hence, these particles (see Figure 1) obtained by a grafting from technique<sup>21–23</sup> represent suitable model systems for studying the solution behavior of spherical polyelectrolyte brushes.

Previously, a number of these system varying with regard to  $L_c$ ,  $\sigma$ , and  $R$  have been studied by dynamic light scattering.<sup>38</sup> By measuring the hydrodynamic radius  $R_H$  of the particles as a function of ionic strength and pH, it could be shown that the polyelectrolyte chains

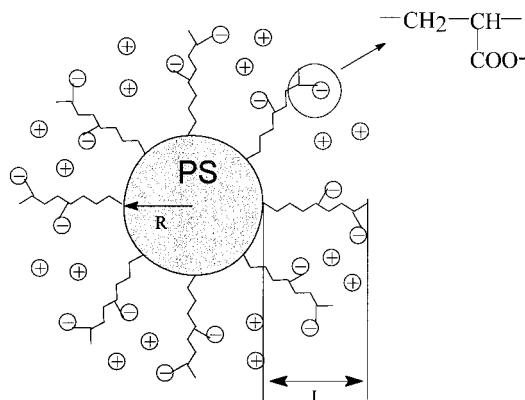


**Figure 1.** Sketch of the spherical polyelectrolyte brushes investigated here: Linear chains of poly(acrylic acid) (PAA) are chemically grafted onto the surface of a colloidal poly(styrene) particle. The contour length  $L_c$  can be determined by cleaving off the chains from the surface and subsequent analysis of the resulting PAA in solution.<sup>37,38</sup> Details of the synthesis and characterization of the spherical polyelectrolyte brushes may be found in refs 37 and 38.

chemically attached to the surface are stretched to nearly full length if the ionic strength is low. The salt concentration within the corona was calculated using the theory of Hariharan et al.<sup>39</sup> which assumes a Donnan equilibrium between the brush layer and the solution. Thus, the counterions are assumed to be confined within the polyelectrolyte brush. This point is well-confirmed by a recent investigation of block copolymer micelles by small-angle neutron scattering (SANS).<sup>34</sup>

In this paper we present the first study of these particles by small-angle X-ray scattering (SAXS).<sup>40</sup> The core of the particles consist of poly(styrene) (PS) which has a low X-ray contrast<sup>41</sup> whereas the corona consists of linear poly(acrylic acid) (PAA) which has a strong X-ray contrast toward water. Hence, the measured scattering originates mainly from the corona of polyelectrolyte chains. Moreover, the contrast of the corona can be enhanced by use of cesium counterions since these ions exhibit a high X-ray contrast in water.

The interaction between the long polyelectrolyte chains is varied systematically by changing the concentration of the particles from the dilute to the concentrated regime. The onset of chain overlap can easily be calculated by estimating the effective volume fraction of the particles in water. This quantity can be derived from the measured hydrodynamic radius of the particles at a given ionic strength.<sup>37</sup> The charges of the chains in the corona can be tuned by adjusting the pH of the system: at low pH the PAA chains are virtually uncharged whereas full dissociation results at pH > 10.<sup>38</sup> Hence, a comparison of charged and uncharged spherical brushes at a given concentration can reveal the features evoked by electrostatic interaction in these systems.

### Evaluation of Scattering Data

The analysis presented here rests on a comparison of the spherical brushes in the uncharged (low pH; cf. ref 38) and the fully charged state (pH > 10; ref 38). It is hence necessary to discuss first the scattering signal to be expected for an uncharged spherical brush. The measured scattering intensity  $I(q)$  of a suspension of noninteracting spherical brushes contains in principle three independent contributions, the origin of which is depicted in Figure 2 (cf. ref 43):

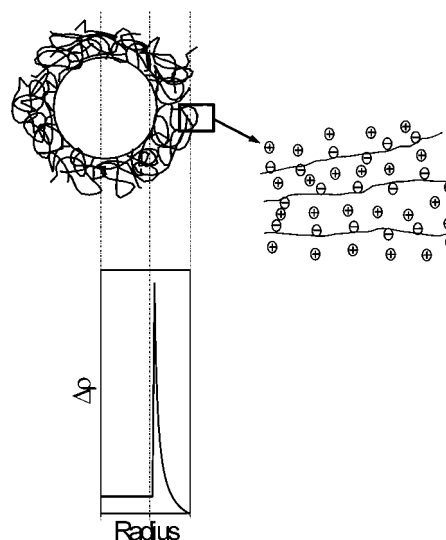


**Figure 2.** Modeling of the measured scattering SAXS intensity: The term  $I_{CS}(q)$  which is dominant at low  $q$  values refers to a core-shell particle with the excess electron density  $\Delta\rho(R)$ . The polymer chains in the corona of the particles exhibit thermal fluctuations which lead to  $I_{fluct}(q)$ . Finally, the poly(styrene) cores of the particles are not entirely homogeneous, but the density of the solid poly(styrene) fluctuates weakly around a mean value. This gives the third term  $I_{PS}(q)$  which gives a contribution to  $I(q)$  that is found negligible compared to the other terms. As discussed in the text, all three contributions to  $I(q)$  derive from statistically independent fluctuations of the electron density in the system. Hence, the respective scattering intensities add up as stated by eq 1.

$$I(q) = I_{CS}(q) + I_{fluct}(q) + I_{PS}(q) \quad (1)$$

Here  $I_{CS}(q)$  is the part of  $I(q)$  due to the core-shell structure of the particles, i.e., the scattering intensity caused by a composite particles having a homogeneous core and a shell. The core and the shell are characterized by a different electron density shown schematically in Figure 1. The shell, however, does not consist of a solid material but of polymer chains. Hence, two contributions to the observed  $I(q)$  are to be expected: At intermediate  $q$  value the typical distances of the order of  $2\pi/q$  are longer than the average distances between the densely packed chains. In this region the small-angle scattering experiment cannot resolve the structure of single polymer chains but only probes the spatial fluctuations of the chains. As already discussed by Auroy and Auvray,<sup>44-46</sup> for the case of flat brushes this contribution may become the leading term at higher  $q$  values and must be taken into account. In the following this part is termed  $I_{fluct}(q)$ .

At highest  $q$  values  $2\pi/q$  has become so small that the SAXS experiment "sees" the local structure of single chains.<sup>47</sup> In this case the measured intensity should scale with  $q^{-1}$  as expected for a rodlike structure (see the discussion of this point by Guenon et al.).<sup>32</sup> It is to be understood, however, that in the case of the dense systems under consideration here this part of  $I(q)$  only comes into play for the highest  $q$  values in which parasitic scattering and other problems of the background may impose severe difficulties for the evaluation of data.<sup>48</sup> Hence, this contribution is dismissed in the present discussion. Finally,  $I_{PS}(q)$  denotes the scattering intensity which is caused by the density fluctuations of the solid PS core of the particles.<sup>41-43,48</sup> It must be understood that all contributions originate from statistically independent fluctuations. Hence, their intensities

will add up because the respective cross-terms will cancel out.

For spherical symmetric particles with radius  $R$  is  $I_{CS}(q)$  equal to  $B^2(q)$  where the scattering amplitude  $B(q)$  is given by<sup>40,41</sup>

$$B(q) = 4\pi \int_0^R [\rho(r) - \rho_m] r^2 \frac{\sin(qr)}{qr} dr \quad (2)$$

Here  $\rho(r) - \rho_m$  denotes the radial excess electron density which has been depicted in Figure 2, and  $\rho_m$  is the electron density of the medium. In the course of the analysis to be conducted here, it is important to realize that  $I_{CS}(q)$  will decrease with  $q^{-4}$  at sufficiently high  $q$  (Porod's law)<sup>40</sup> if the core-shell particles have sharp interfaces. For particles with diffuse interfaces  $I_{CS}(q)$  will diminish even stronger at high  $q$ .<sup>40</sup> Model calculations and previous experimental studies on core-shell particles therefore suggest that  $I_{CS}(q)$  of the present particles will decrease by 2–3 orders of magnitude in the range  $0 < q < 0.2 \text{ nm}^{-1}$ . Equation 2 can easily be generalized to include polydisperse systems of noninteracting systems.<sup>41</sup> In this case the intensities  $B_i^2(q)$  of the species  $i$  are added up weighted by their respective number density  $N_i$ .

The second term  $I_{\text{network}}(q)$  may be described in good approximation by a Lorentzian since it is due to the thermal fluctuations of a semiconcentrated polymer solution<sup>49</sup>

$$I_{\text{fluct}}(q) = \frac{I_{\text{fluct}}(0)}{1 + \xi^2 q^2} \quad (3)$$

In this context  $I_{\text{in}}(0)$ ,  $I_{\text{fluct}}(0)$ , and  $\xi$ , the correlation length of the spatial fluctuations, are treated as adjustable parameters.

The third term of eq 1,  $I_{\text{PS}}(q)$ , is the small but nonnegligible contribution to  $I(q)$  caused by the density fluctuations of the solid PS core. This term and its magnitude have been discussed at length recently in the course of the SAXS analysis of composite latex particles.<sup>41,43,48</sup>

The decomposition of the experimental scattering intensities can be done as follows: It is evident that  $I_{CS}(q)$  will dominate  $I(q)$  at small  $q$ . This is due to the fact that  $I_{CS}(q)$  refers to the entire core-shell particle, the diameter of which is between 120 and 160 nm. This also implies that  $I_{CS}(q)$  will decrease most rapidly with increasing  $q$  as discussed above. The correlation length  $\xi$  governing  $I_{\text{fluct}}(q)$  is expected to be of the order of a few nanometers for the system under consideration here. As discussed above,  $I_{\text{fluct}}(q)$  may be neglected at small  $q$  to good approximation. As a consequence of this,  $I(q)$  measured up to  $q \approx 0.2 \text{ nm}^{-1}$  can be described solely by  $I_{CS}(q)$  while all other terms may be dismissed in this  $q$  range. On the other hand,  $I_{CS}(q)$  will be greatly diminished for  $q > 0.2 \text{ nm}^{-1}$  and  $I_{\text{fluct}}(q)$  will become the leading term at higher scattering angle because it scales with  $q^{-2}$  for large  $q$  values. The subtraction of  $I_{\text{PS}}(q)$  provides no difficulty because this term can be determined from SAXS measurements of the PS core latex. By virtue of these propitious facts, a decomposition of  $I(q)$  into the three terms of eq 1 becomes possible.

The presence of several contributions to  $I(q)$  restricts the angular range in which  $I_{CS}(q)$  can be analyzed. This problem has been discussed in detail in a previous analysis of polymeric layers attached to the surface of

latex particles by SAXS.<sup>47</sup> Here it turned out that only lower moments of the distribution  $\rho(r) - \rho_m$  are available. Therefore, no conclusion can be drawn about its exact dependence of  $\rho(r) - \rho_m$  on  $r$ .

If the charges within the corona are fully dissociated, the chains will be strongly stretched depending on the ionic strength as discussed for the present system in great detail.<sup>38</sup> Hence, both  $I_{CS}(q)$  and  $I_{\text{fluct}}(q)$  will be affected. In addition, there may be fluctuations of the distribution of the counterions as well. Because of the restricted  $q$  range, however, SAXS is only sensitive to the internal region of the brush in which the density of the chains is highest. Hence, the overall dimensions of the brush can only be determined securely by DLS.

The extension of the surface layer at high pH will lead to a much higher effective volume fraction. This must be followed by a strong spatial correlation of the particles as expressed through the structure factor  $S(q)$ .<sup>40,41</sup> The alterations effected on the measured scattering intensity, however, are visible only in the region of smallest  $q$  values and can hardly be resolved by the present SAXS experiments.

## Experimental Section

The spherical polyelectrolyte brushes employed in this study were prepared as described in refs 37 and 38 by photoemulsion polymerization. The system studied here was latex L15 of ref 38. This system is characterized by the following parameters:  $R = 66 \text{ nm}$  (determined by DLS),  $L_c = 228 \text{ nm}$ ,  $\sigma = 0.039 \text{ nm}^{-2}$  (see ref 38). A separate analysis of the core particles by SAXS leads to a slightly smaller diameter (58 nm). After purification of the latex a pH of 11 adjusted through addition of CsOH.

Most of the SAXS measurements presented have been conducted using the improved Kratky camera described recently.<sup>42</sup> The raw data have been corrected for the scattering of the serum and of the sample holder. Desmearing of the scattering curves was done as described in refs 41 and 42. In all cases to be discussed here absolute scattering intensities have been obtained. For better comparison with SANS data all intensities are expressed in  $\text{cm}^{-1}$ .

Additional SAXS data have been measured using the ID02A beamline of the ESRF in Grenoble. Measurements of well-characterized latexes demonstrated that both the Kratky camera and the ID02A came to the same  $I(q)$  within  $0.02 < q$ .

## Results and Discussion

As depicted in Figure 1, the spherical polyelectrolyte brushes consist of a solid PS core of 58 nm (determined by SAXS) with attached chains of poly(acrylic acid) (PAA). The corona consists therefore of an annealed brush, and the charges depend strongly on the pH in the system. This point has been investigated by dynamic light scattering in great detail, and the results are gathered in ref 38. Here it could be demonstrated that the fully charged state can be reached at a pH  $> 10$ . This limits the lowest ionic strength attainable to approximately  $10^{-3}$ , but the corona may be treated as a quenched brush. Since all experiments to be discussed here are done at rather high concentration ( $> 1 \text{ wt } \%$ ), the ionic strength will be governed mainly by the particles themselves, and shifting the pH to ca. 10 imposes no problem.

To assess the information gained from SAXS experiments, it is necessary to discuss first  $I(q)$  obtained at low pH (pH ca. 3). Here the PAA chains are only weakly charged, and the entire particle may be treated as a neutral spherical brush. Figure 3a,b gives the resulting scattering intensity together with the fit of eq 1. The scattering contributions of the polyelectrolyte chains



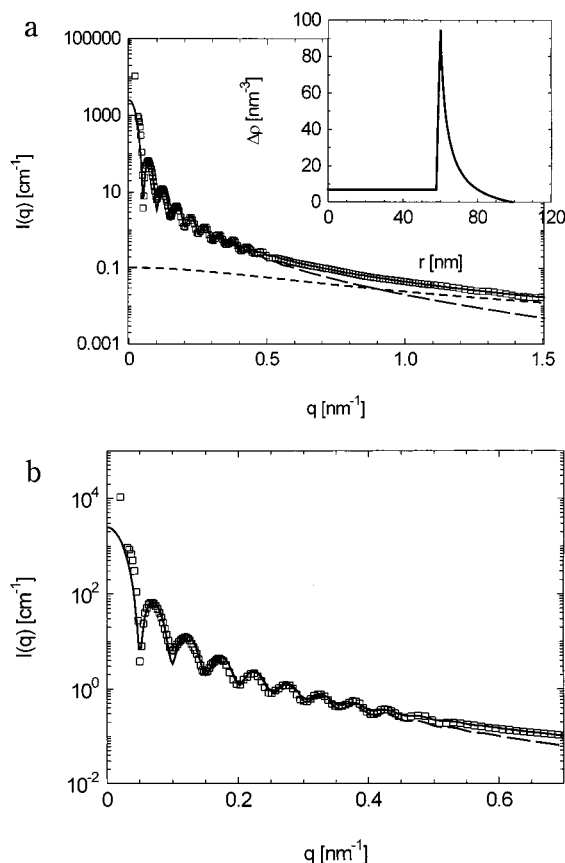
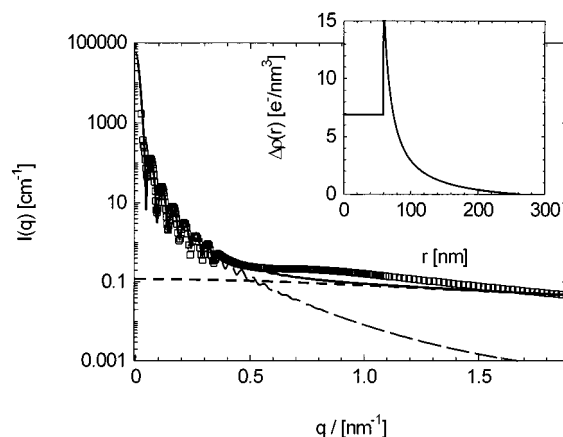


**Figure 3.** Scattering intensity  $I(q)$  of the spherical polyelectrolyte brushes at low pH, i.e., in the virtually uncharged state as a function of the magnitude of the scattering vector  $q$ . The weight concentration of the particles is 12 wt %. (a) Survey of the contributions according to eq 1. The squares mark the measured intensity whereas the long-dashed line give the contribution  $I_{CS}(q)$  discussed in conjunction with Figure 2. The respective profile of the radial excess electron density is displayed in the inset. (b) An enlarged view of the small-angle region of  $I_{CS}(q)$ . The short-dashed line in (a) gives  $I_{fluct}(q)$  (see eq 3). The solid line shows the modeled intensity according to eq 1.

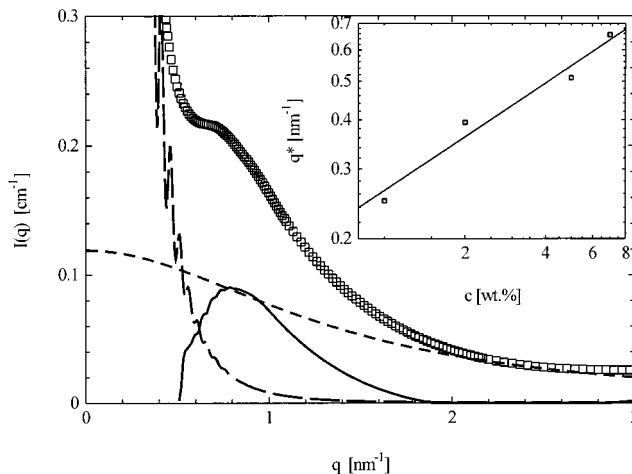
and their counterions are very strong up to the highest  $q$  values, and  $I_{PS}(q)$  can be disregarded in the course of the present discussion.

Figure 3a shows the entire  $q$  range evaluated. The strong oscillations of  $I_{CS}(q)$  are clearly visible at small  $q$  values and show the narrow size distribution of the particles. The region of small  $q$  together with the fits of eq 2 in this range is shown separately in Figure 3b. The restricted  $q$  range does not allow a detailed analysis of the excess electron distribution of the corona because  $I_{fluct}(q)$  becomes the leading term for  $q > 1 \text{ nm}^{-1}$ . For the present discussion it suffices, however, to describe the data at small  $q$  by assuming an exponentially decaying profile shown in the inset of Figure 3a. This profile is suggested by previous analyses of spherical particles having linear polymer chains attached on the surface.<sup>48,50</sup> The outer limit of the profile has been equated to the hydrodynamic radius determined by DLS. Figure 3b demonstrates that an excellent fit is achieved under these premises.

At  $q > 1 \text{ nm}^{-1}$   $I_{fluct}(q)$  becomes the leading term, and the parameters of eq 3 have been determined by fits taking only data beyond  $q = 1.5 \text{ nm}^{-1}$ . From this fit a correlation length of  $\xi$  of the order of 1–2 nm results, which is a reasonable value. With these terms the entire  $q$  range may be described as demonstrated by Figure 3.



**Figure 4.** Scattering intensity  $I(q)$  of the spherical polyelectrolyte brushes at high pH (11), i.e., in the fully charged state as a function of the magnitude of the scattering vector  $q$ . The weight concentration of the particles is 12 wt %. The squares mark the measured intensity whereas the long-dashed line gives the contribution  $I_{CS}(q)$  discussed in conjunction with Figure 2. The respective profile of the radial excess electron density is displayed in the inset. The short-dashed line gives  $I_{fluct}(q)$  (see eq 3). The solid line shows the modeled intensity according to eq 1.



**Figure 5.** Enlarged view of the peak in  $I(q)$  due to the interaction of the chains grafted to the spherical latex particles. Note the linear scale of the ordinate. The squares mark the measured intensity whereas the long-dashed line give the contribution  $I_{CS}(q)$  discussed in conjunction with Figure 2. The short-dashed line in Figure 3a gives  $I_{fluct}(q)$  (see eq 3). The solid line shows the  $I(q) - I_{CS}(q) - I_{fluct}(q)$ .

Figure 4 displays the SAXS intensities obtained for particles at pH = 11. Here the polyelectrolyte chains are fully charged, and DLS measurements showed the strong stretching of corona.<sup>38</sup> It must be noted that the concentration employed in the SAXS measurements is 12 wt %, which is higher by 2 orders of magnitude than the concentrations used for DLS measurements. At these high concentrations the chains of the corona of different particles must overlap considerably. Figure 4 demonstrates that the consequence of this overlap is a new peak which for this particular concentration is located at  $q \approx 0.9 \text{ nm}^{-1}$ . The peak is even better visible in Figure 5, which displays an enlarged view of the scattering intensity. No model of the radial density of the particles could possibly explain the maximum of  $I(q)$  in this angular region. This is borne out directly from the previous analysis of the  $I(q)$  measured from uncharged particles.

To elucidate the origin of the peak seen in Figures 4 and 5, the following experiments have been done:

(i) Measurements done at lower concentrations demonstrate that the peak is shifted to smaller  $q$  values and finally vanishes for concentrations smaller than 1 wt %. It is thus evident that it must be related to the interaction of the particles and not to the internal structure of the corona. The position of the peak can directly be taken from the graph and is found to vary with the square root of particle concentration (cf. also below).

(ii) Adding salt to the suspensions lowers the peak considerably. No effect is visible anymore if 0.5 M NaCl is added to the system.

These findings demonstrate that the effect must be related to the electrostatic interaction of the particles and occurs only at sufficiently low ionic strength. This is very similar to what is found in solutions of linear polyelectrolytes: Here the "polyelectrolyte peak" is visible only at low salinity and shifts to smaller  $q$  values if the polyelectrolyte concentration is lowered.<sup>4,12–15</sup>

From these findings we conclude that it has the same origin which must be located in the virtually unscreened interaction of the strongly charged polyelectrolyte chains. From what is known about the case of free polyelectrolyte chains one must assume that the chains exhibit a preferred distance and hence some local order leading to the observation of a peak in  $I(q)$ . Obviously, the order thus inferred cannot have a long range but must be envisaged as a short-range, liquidlike arrangement of the chains between the spheres.

To investigate this unexpected finding in more detail, the measured scattering curves have been decomposed into the contributions of eq 1 and an additional signal due to the interaction of the chains attached to the surface of the particles. This procedure assumed that the intensities of all contributions add up independently; that is, there is no cross-term between these terms. While this is fully justified for the terms enumerated in eq 1, it is less obvious that this procedure is admissible to the additional signal deriving from the interaction of chains located on different particles. If one assumes in first approximation that the positions of the partially ordered regions in which the chains exhibit some liquidlike order are not correlated to the centers of gravity of the particles, all cross-terms vanish in average. In this case the signal of the partially ordered regions adds up independently to the contributions already discussed above (cf. the discussion of eq 1).

Figure 5 displays the resulting decomposition for the data shown in Figure 4. It is clear that subtracting all contributions according to eq 1 from the measured  $I(q)$  leads to a distinct scattering signal with a well-defined maximum (solid curve in Figure 5). We do not attach too much significance to the form of this signal, however, but only discuss the dependence of the position  $q^*$  of the maximum on particle concentration. The inset displays  $q^*$  as a function of the concentration of spherical polyelectrolyte brushes. The solid line in the inset has a slope of 0.45 whereas a slope of 0.5 was already found by taking the position of the maximum directly from the scattering curves. Within the present limits of errors this comes close to the value of 0.5 found for semidilute solutions of free polyelectrolyte chains (see above).

## Conclusion

We have demonstrated for the first time that the interaction of highly charged polyelectrolyte chains leads to the same ordering phenomena seen in solutions of free polyelectrolyte chains of the same concentration. The correlation is seen from a distinct signal in the scattering curves which vanishes if an excess of low-molecular-weight salt is added. The position  $q^*$  of the maximum scales approximately with the square root of the particle concentration which is directly related to the concentration of the polyelectrolyte chains. A similar phenomenon has very recently been observed for solutions of charged star polymers<sup>51</sup> and for micelles with charged coronae.<sup>52</sup> Hence, the "polyelectrolyte peak" seems to be a more general phenomenon and points to a general mechanism of interparticular correlation induced by strong electric charges.

**Acknowledgment.** Financial support by the Deutsche Forschungsgemeinschaft, Schwerpunkt Polyelektrolyte, is gratefully acknowledged.

## References and Notes

- (1) Mandel, M. Polyelectrolytes. In *Encyclopedia of Polymer Science and Engineering*, 2nd ed.; Mark, F. H., Bikales, N. M., Overberger, C. G., Menges, G., Eds.; Wiley: New York, 1988; Vol. 11, p 739.
- (2) Oosawa, F. *Polyelectrolytes*; Marcel Dekker: New York, 1971.
- (3) Katchalsky, A. *Pure Appl. Chem.* **1971**, *26*, 327.
- (4) Schmitz, K. S. *Macroions in Solution and in Colloidal Suspension*; VCH Publishers: New York, 1993.
- (5) Förster, S.; Schmidt, M. *Adv. Polym. Sci.* **1995**, *120*, 51.
- (6) Hayter, J.; Jannink, G.; Brochard, F.; de Gennes, P.-G. *J. Chem. Phys.* **1980**, *41*, L451.
- (7) Hess, W.; Klein, R. *Adv. Polym. Sci.* **1982**, *32*, 173.
- (8) Vilgis, T.; Borsali, R. *Phys. Rev. A* **1991**, *43*, 6857.
- (9) Weyerich, B.; D'Aguzzo, B.; Canessa, E.; Klein, R. *Faraday Discuss. Chem. Soc.* **1990**, *90*, 245.
- (10) Nierlich, M.; Williams, C. E.; Boué, F.; Cotton, J. P.; Farnoux, B.; Jannink, G.; Picot, C.; Moan, M.; Wolff, C.; Rinaudo, M.; de Gennes, P.-G. *J. Phys. (Paris)* **1979**, *40*, 701.
- (11) Drifford, M.; Dalbiez, J. P. *J. Phys. Chem.* **1984**, *88*, 5368.
- (12) Förster, S.; Schmidt, M.; Antonietti, M. *Polymer* **1990**, *31*, 781.
- (13) Sedlak, M.; Amis, E. *J. Chem. Phys.* **1992**, *96*, 817.
- (14) Borsali, R.; Nguyen, H.; Pecora, R. *Macromolecules* **1998**, *31*, 1548.
- (15) Ermi, B. D.; Amis, E. J. *Macromolecules* **1998**, *31*, 7378.
- (16) Fleer, G. J.; Cohen Stuart, M. A.; Scheutjens, J. M. H. M.; Cosgrove, T.; Vincent, B. *Polymers at Interfaces*; Chapman and Hall: London, 1993.
- (17) Pincus, P. *Macromolecules* **1991**, *24*, 2912.
- (18) Zhulina, E. B.; Borisov, O. V.; Birshtein, T. M. *J. Phys. II* **1992**, *2*, 63.
- (19) Borisov, O. V.; Zhulina, E. B.; Birshtein, T. M. *Macromolecules* **1994**, *27*, 4795.
- (20) Zhulina, E. B.; Birshtein, T. M.; Borisov, O. V. *Macromolecules* **1995**, *28*, 1491.
- (21) Prucker, O.; Rühle, J. *Macromolecules* **1998**, *31*, 592.
- (22) Prucker, O.; Rühle, J. *Macromolecules* **1998**, *31*, 602.
- (23) Prucker, O.; Schimmel, M.; Tovar, G.; Knoll, W.; Rühle, J. *Adv. Mater.* **1999**, *10*, 1073.
- (24) Biver, C.; Hariharan, R.; Mays, J.; Russel, W. B. *Macromolecules* **1997**, *30*, 1787.
- (25) Hariharan, R.; Biver, C.; Mays, J.; Russel, W. B. *Macromolecules* **1998**, *31*, 7506.
- (26) Ahrens, H.; Förster, S.; Helm, Ch. A. *Phys. Rev. Lett.* **1998**, *81*, 4172.
- (27) Tran, Y.; Auroy, P.; Lee, L.-T. *Macromolecules* **1999**, *32*, 8952.
- (28) Tran, Y.; Auroy, P.; Lee, L.-T.; Stamm, M. *Phys. Rev. E* **1999**, *60*, 6984.
- (29) Astafieva, I.; Zhong, X. F.; Eisenberg, A. *Macromolecules* **1993**, *26*, 7339.
- (30) Khougaz, K.; Astafieva, I.; Eisenberg, A. *Macromolecules* **1995**, *28*, 7135.
- (31) Guenoun, P.; Delsanti, M.; Gazeau, D.; Mays, J. W.; Cook, D. C.; Tirrell, M.; Auvray, L. *Eur. Phys. J. B* **1998**, *1*, 77.

- (32) Guenon, P.; Muller, F.; Delsanti, M.; Auvray, L.; Chen, Y. J.; Mays, J. W.; Tirrell, M. *Phys. Rev. Lett.* **1998**, *81*, 3872.
- (33) Shusharina, N. P.; Linse, P.; Khokhlov, A. R. *Macromolecules* **2000**, *33*, 3892.
- (34) Groenewegen, W.; Lapp, A.; Egelhaaf, S. U.; van der Maarel, J. R. C. *Macromolecules* **2000**, *33*, 4080.
- (35) Klein Wolterink, J.; Leermakers, F. A. M.; Fleer, G. J.; Koopal, L. K.; Zhulina, E. B.; Borisov, O. V. *Macromolecules* **1999**, *32*, 2365.
- (36) Mays, J. W. *Polym. Commun.* **1990**, *31*, 170.
- (37) Guo, X.; Weiss, A.; Ballauff, M. *Macromolecules* **1999**, *32*, 6043.
- (38) Guo, X.; Ballauff, M. *Langmuir*, in press.
- (39) Hariharan, R.; Biver, C.; Russel, W. B. *Macromolecules* **1998**, *31*, 7514.
- (40) Glatter, O.; Kratky, O., Eds.; *Small Angle X-ray Scattering*; Academic Press: London, 1982.
- (41) Dingenouts, N.; Bolze, J.; Pötschke, D.; Ballauff, M. *Adv. Polym. Sci.* **1998**, *144*, 1.
- (42) Dingenouts, N.; Ballauff, M. *Acta Polym.* **1998**, *49*, 178.
- (43) Dingenouts, N.; Norhausen, Ch.; Ballauff, M. *Macromolecules* **1998**, *31*, 8912.
- (44) Auroy, P.; Auvray, L. *J. Phys. II* **1993**, *3*, 227.
- (45) Auroy, P.; Auvray, L. *Langmuir* **1994**, *10*, 225.
- (46) Auroy, P.; Auvray, L. *Macromolecules* **1996**, *29*, 337.
- (47) Pötschke, D.; Hickl, P.; Ballauff, M.; Åstrand, P.-O.; Pedersen, J. S. *Macromol. Theory Simul.* **2000**, *9*, 345.
- (48) Seelenmeyer, S.; Ballauff, M. *Langmuir* **2000**, *16*, 4094.
- (49) de Gennes, P.-G. *Scaling Concept in Polymer Physics*; Cornell University Press: Ithaca, NY, 1979.
- (50) Mears, S. T.; Cosgrove, T.; Obey, T.; Thomson, L.; Howell, I. *Langmuir* **1998**, *14*, 4997.
- (51) Rawiso, M., private communication.
- (52) Guenon, P., private communication.

MA001373N